3D-Printed Flexible Tactile Sensor Mimicking the Texture and Sensitivity of Human Skin

*Haihang Wang, Hongmei Yang, Sheng Zhang, Li Zhang, Jiusheng Li, and Xiangqiong Zeng**

The development of 3D printing technology toward multifunction devices may affect various fields from intelligent systems and wearable electronic devices to energy storage and flexible light-emitting devices. A new type of piezoresistive sensor is designed by mimicking the texture and sensitivity of human skin. It is fabricated by 3D printing with a new kind of ink that is composed of interconnected polydimethylsiloxane microspheres (MPs) with carbon nanotubes distributed on their surfaces. This structure gives an electronic skin fabricated from these sensors modulus similar to that of human skin; furthermore, it elastically deforms under external forces. The response of the electronic skin to shear forces is evaluated by simulating the touch behavior of human skin, and it is found that the tactile sensors are sensitive to applied shear forces. They demonstrate sensitivity as low as 2.08 kPa^{-1} at a pressure of just 0.12 kPa, with short response time (50 ms), high durability (over 8000 cycles), and flexibility.

1. Introduction

Recently, stretchable electronic devices have attracted far-ranging attention due to their great potential applications in various engineering applications, such as wearable electronics, intelligent systems,[1–6] flexible light-emitting devices,[7–9] energy harvesting devices,[10–14] stretchable displays, etc.[15–17] In the last decade, the research of flexible electronic devices and wearable sensors has significantly accelerated as a result of progress in new materials and advanced manufacturing. For wearable electronics, the mechanical flexibility and scalability of the device, interfacial mechanics and chemical properties, and the ability to maintain the superior properties of the devices are essential factors to consider. One of the most common methods being used for wearable flexible electronic devices to achieve excellent stretchability is to change the shape factors in the structure of wearable electronic devices. Other methods include utilizing flexible material composites with conductive nanomaterials and conductive coating materials to make stretchable matrix.

As the human skin plays an important role in our interaction with the outside environment, wearable flexible electronic devices that mimic the functions of human skin by converting stimuli signals into electronic signals could have great significance for prosthetics and medicine.[18,19] One of the most common methods being used for measuring tactile stimuli is to employ piezoresistive mechanisms.[20,21] When a force is applied to the tactile sensor, the piezoresistive sensor converts the mechanical strain into an impedance change. In recent years, piezoresistive sensors have been widely used in many fields due to their sensitivity to both flexion and pressure, simple read-out mechanism. For wearable electronics sensor, sensitivity, linearity range, response time, cyclability, detection limit, power consumption, and stability are essential factors to consider.[4,22–27] In particular, sensitivity is probably the most important factor of the sensor. The sensitivity of the piezoresistive tactile sensor is defined as the ratio of change in the resistance to the change in the applied pressure ($S = dR/dP$, where P is the applied pressure on the sensor and R is the measured resistance.). Recently, researchers explore some different method to fabricate high sensitivity wearable sensors. The modulation of the microstructure of the material is the simplest and most effective way for the manufacture of tactile sensors. For tactile sensors, a small applied force can cause subtle structural changes.[20,21,28–31] Moreover, modulate the contact resistance between the active

H. H. Wang, H. M. Yang, Prof. J. S. Li, Prof. X. Q. Zeng
Laboratory for Advanced Lubricating Materials
Shanghai Advanced Research Institute
Chinese Academy of Sciences
Shanghai 201210, China
E-mail: zengxq@sari.ac.cn
H. H. Wang, H. M. Yang
University of Chinese Academy of Sciences
Beijing 100049, China
Dr. S. Zhang
Division of Biomedical Engineering
Renal Division
Department of Medicine
Brigham and Women's Hospital
Harvard Medical School
Cambridge, MA 02139, USA
Dr. S. Zhang
Micro/Nano Technology Center
Tokai University
Hiratsuka 259-1292, Japan
Dr. L. Zhang
School of Information and Management
Shanghai Lixin University of Accounting and Finance
Shanghai 201209, China
The ORCID identification number(s) for the author(s) of this article can be found under https://doi.org/10.1002/admt.201900147.

DOI: 10.1002/admt.201900147

layer and the electrode through compress is also an effective method to improve the sensitivity.[29,32,33] By applying such a strategy, Gong et al.[34] fabricated a high sensitivity pressure sensor by coating Au nanowires on paper and the sensitivity of the pressure sensor is 1.14 kPa^{-1}. Besides, Huang et al.[35] fabricated a millefeuille-like architecture pressure sensor by reduced graphene oxide and the sensitivity of the pressure sensor is 0.82 kPa^{-1}. Pan et al.[36] present an ultrasensitive piezoresistive pressure sensor by using a porous conductive polymer thin film and the sensitivity of the pressure sensor is 133.1 kPa^{-1} in the low-pressure regime (<30 Pa). However, previous research mainly focused on traditional 2D planar fabrication techniques, such as lithography, rotary coating, and metal deposition.[36,37] These potentially limit the application of these technologies to the field where the fabrication of devices is only needed raw materials on site. Therefore, researchers attempt to fabricate wearable sensors and electronic skin using a direct 3D printing method. Guo et al.[38] present a new kind of stretchable electronic skin by 3D printing under ambient conditions and Wei et al.[39] report using 3D printing to fabricate freestanding wavy electrodes and the stretchability is as high as 315%. In addition, Roh et al.[40] present a new type of capillary suspension ink for 3D printing and the ink contains polydimethylsiloxane (PDMS) microspheres (MPs) and uncured PDMS liquid precursor.

2. Results and Discussion

The above researches indicate that microstructure is essential to achieve desired sensing characteristics. Therefore, in the present research, we presented the design and manufacture of a new type of piezoresistive sensors that were 3D printed by a new kind of 3D printing ink. For this purpose, we developed a new kind of 3D printing ink, which composed of three ingredients: PDMS MPs, uncured PDMS-CNTs (carbon nanotubes) composite liquid precursor, and water-based medium. The concept diagram of preparing these PDMS-CNT composite inks was described in **Figure 1**a. The active layer of the electronic skin consisted of interconnected PDMS MPs and CNTs distributed on the surface of the MPs. And this material design was the key innovation in this research. The PDMS MPs employed in our experiment enabled the electronic skin to elastically deform under external forces. The PDMS MPs structure improved the contact stability, thereby promoting stability and reproducibility of the flexible tactile sensor. The fabrication process was as following. First, a PDMS emulsion was formed due to the phase separation between the aqueous and organic components, which was confirmed by the optical microscope measurements (Figure S1, Supporting Information). Precured PDMS MPs were prepared by thermal curing of PDMS emulsion at 85 °C for 2 h. The precured PDMS MPs were then added into the uncured

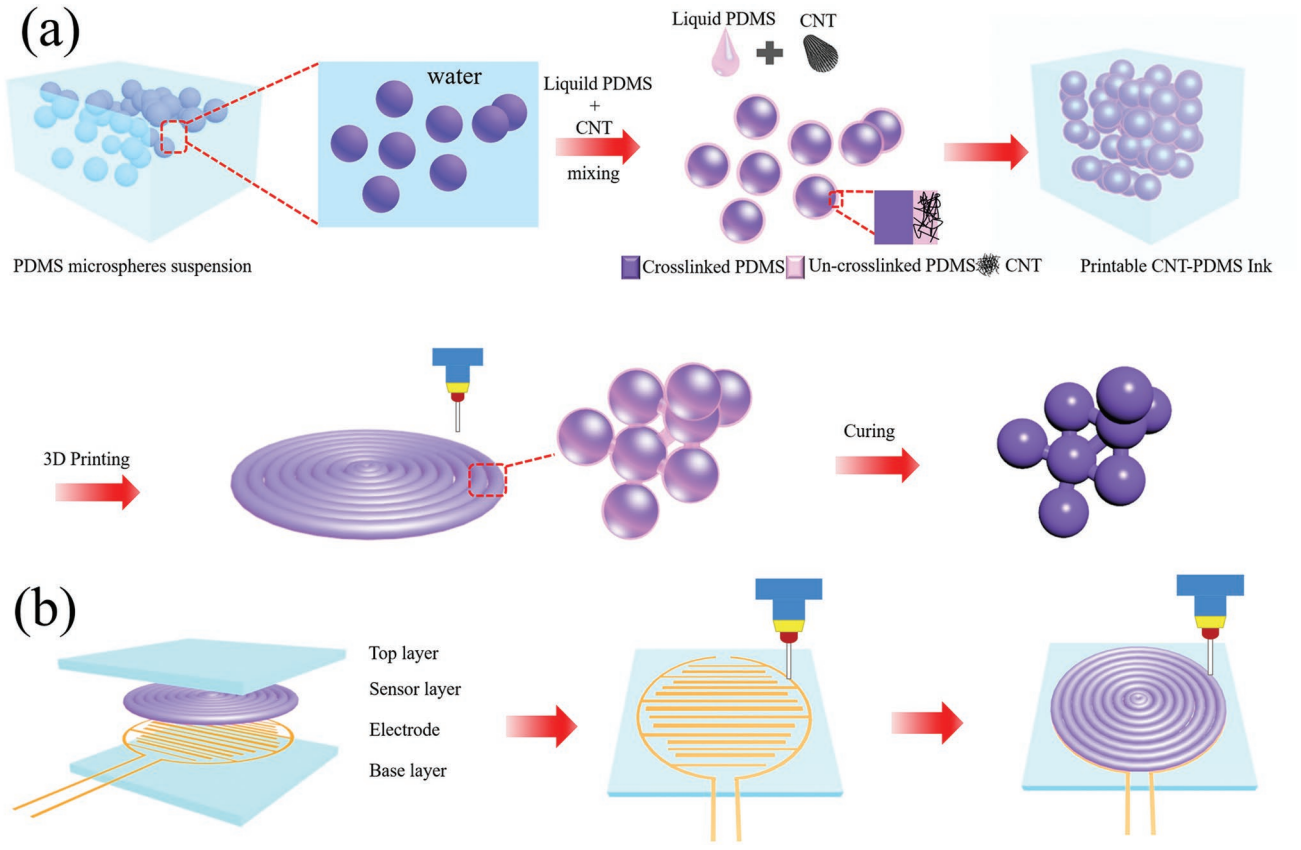

Figure 1. Flexible tactile sensor design conception and procedure of 3D printing. a) The conceptual schematic view of the overall procedure for making these PDMS-CNT composite inks. b) Schematic illustration of the flexible tactile sensor composed of a base layer, electrodes, and a sensor layer.

PDMS-CNTs composite liquid precursor with mechanical stir and then homogenized, thereby promoting wetting of the MPs with uncured PDMS-CNTs composite liquid precursor. The relative amount of the 3D printing ink was optimized according to ink rheological properties and it was found that the best 3D printing results could be obtained with the liquid PDMS/PDMS MPs weight ratio of 1/4. The elastomeric 3D printing ink could be extruded and printed into 3D shapes. Then printed 3D structures were further curing at 60 °C for 5 h. A scanning electron microscope image (SEM; **Figure 2**b) shows the morphology of the MPs in the ink before and after the addition of uncured PDMS-CNTS liquid, which indicated that ink was consisted of interconnected MPs with polydispersing diameters ranging from several microns to tens of microns. Our MPs synthetic approach was tunable because the electronic skin with MPs of different diameters, different size dispersions could be prepared by choosing a different rate of homogenization mixing (Figure S2, Supporting Information). Here, we fabricated flexible tactile sensors by mimicking the texture of human fingers through a continuous 3D printing process. Then we measured the sensing behavior of the tactile sensors. The concept diagram of flexible tactile sensors was shown in Figure 1b.

PDMS-CNTs composite liquid precursor distributed on the surface of the PDMS MPs was confirmed by the SEM images of PDMS MPs before and after uncured PDMS-CNTs composite liquid addition (Figure 2a,b). The wetting of the PDMS

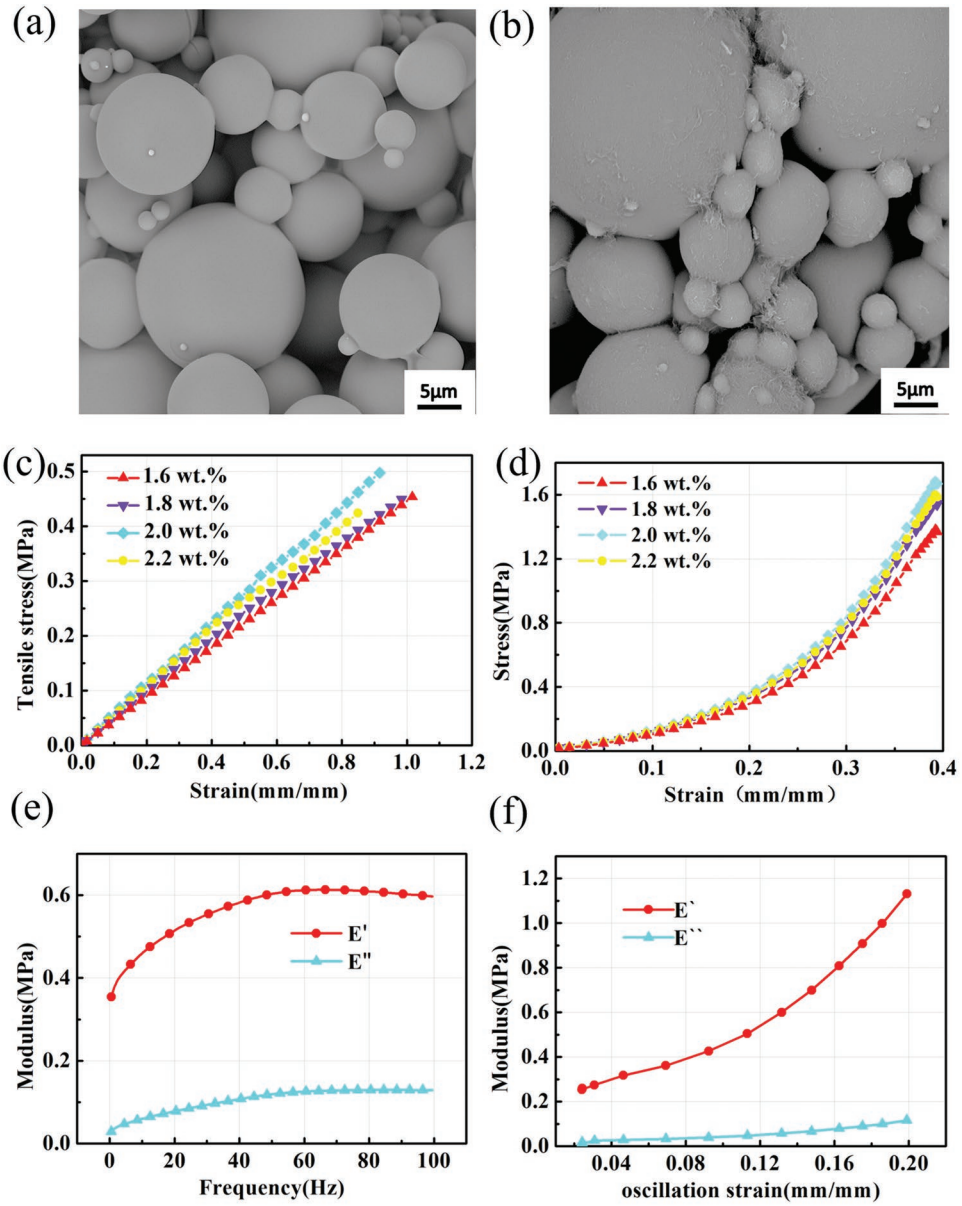

Figure 2. The structure and mechanical behavior of various inks. SEM images of PDMS MPs a) before and b) after uncured PDMS-CNTs composite liquid addition. c) Tensile and d) compressive curve test on the cured MPs inks with different CNTs contents. e) Dynamic modulus of the cured inks with 2.0 wt% CNTs contents. Storage modulus (*E*′) and Loss modulus (*E*″) versus frequency. f) Storage modulus (*E*′) and Loss modulus (*E*″) versus oscillation strain.

MPs with PDMS-CNTs composite liquid precursor was due to the strong affinity, which was attributed to the similarity in chemical composition. That is, as both bases were siloxanes, the MPs were easily wetted by the PDMS-CNTs composite liquid precursor. To study the mechanical properties of the electronic skin, we measured the tensile stress and compressive stress as a function of strain. As shown in Figure 2c, with the decreasing of CNT content, the stretchability of the cured inks increased from 85% to 103%. However, the modulus increased first with the increasing of CNT content, and then decreased when the content of CNT was over 2.0 wt%. This phenomenon may be because when the content of CNTs exceeded 2.0 wt%, the CNTs began to agglomerate, resulting in reduced binding force between the MPs and decreased modulus of the cured inks. Therefore, the optimum CNTs concentration was 2.0 wt% (Figure 2c,d). Besides, the modulus was with minimal effect by the size of MP (Figure S3, Supporting Information). We also carried out dynamic mechanical analyses for the electronic skin to determine its mechanical response under dynamic forces. The storage (E') moduli and loss (E'') moduli as a function of oscillation strain were shown in Figure 2f. The loss and storage moduli both increased as the oscillation strains increased from 0 to 0.2. On the other hand, with the increasing of dynamic frequencies, the loss modulus slightly increased, which was a typical viscoelastic behavior, similar to that of human skin (Figure 2e,f and Figure S4, Supporting Information). Moreover, the measured modulus of the electronic skin was in the range of 0.4–0.6 MPa, which was similar to that of human skin as well (Young's modulus ≈ 0.13–0.66 MPa),[41] suggesting the strain of electronic skin could be highly consistent with that of human skin and reflect the strain of skin accurately. So that the electronic skin could adapt to the skin strain associated with physical movement and could improve the comfort feeling when wearing it.

As shown in **Figure 3**a,b, we fabricated the flexible tactile sensors by mimicking the texture of human fingers. The

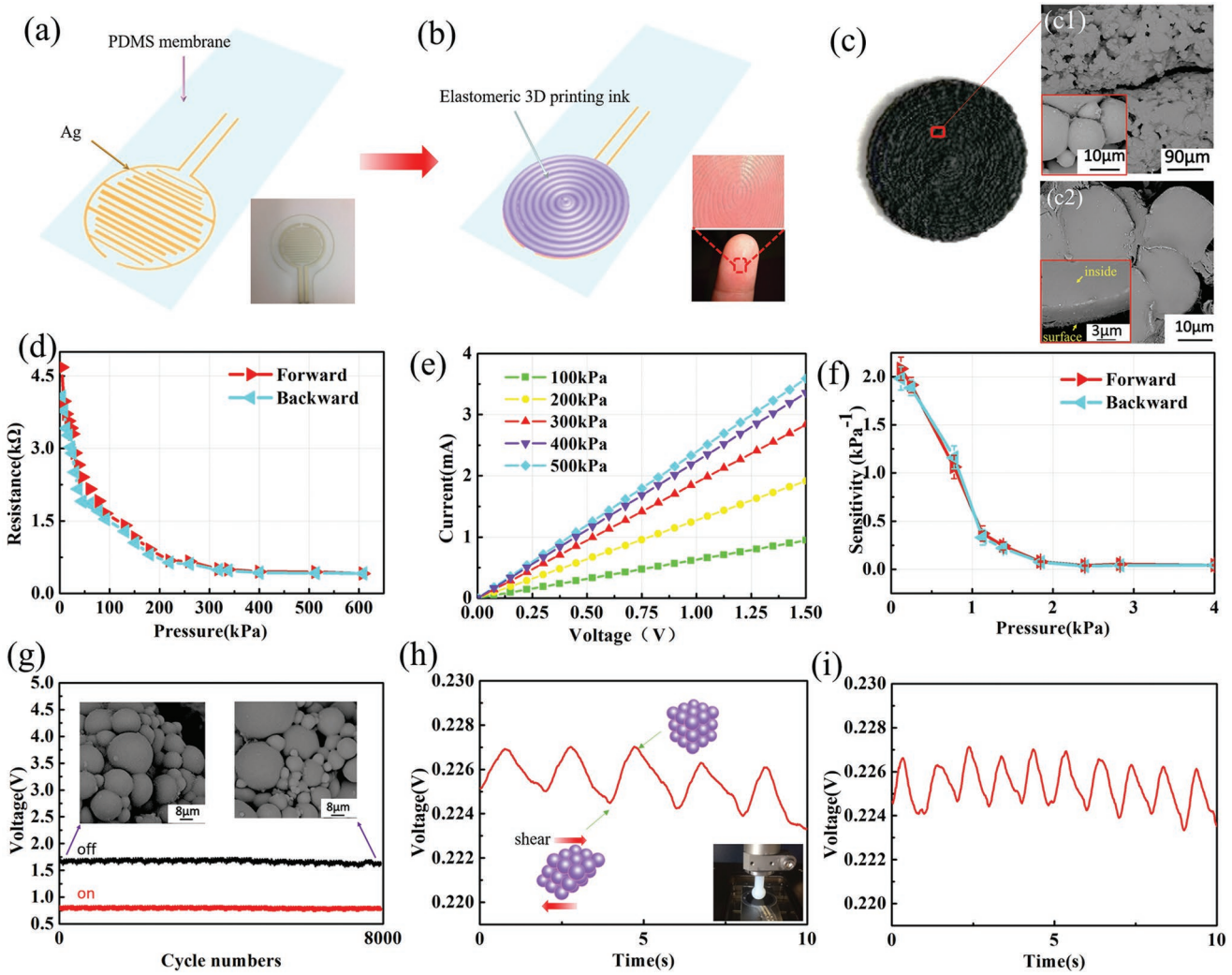

Figure 3. a,b) Schematic diagram of the preparation process of pressure-sensing. c1) The microscope image of the 3D printed microstructures. c2) The cross-section of the PDMS MPs. d) Resistance response of the tactile sensor. e) Current–voltage characteristics of the flexible tactile sensor to different pressures. f) Sensitivity of the pressure sensor. g) Resistance of the pressure sensor over 8000 cycles. The relative voltage changes were responses under h) 0.5 and i) 1 Hz cyclic applied shearing force.

texture of the active layer of the flexible tactile sensor was printed by ejecting through a nozzle with the inner diameter ≈300 μm, which was similar to the fingerprint of human fingers (Figure S5, Supporting Information). SEM images of the active layer of the sensor in Figure 3c showed the microstructure of two adjacent lines and the surface topography of each line (Figure 3c1), which was consisted of distributed PDMS MP. To identify the dispersion of CNTs at the surface of the PDMS MP, we made an SEM image of the cross-section of the active layer of the sensor (Figure 3c2), which displayed the cross-section of the PDMS MPs, and the inset figure confirmed that CNTs were distributed around the surface of each MP. The electrical properties of the flexible tactile sensors with 2.0% CNTs content were analyzed. As the pressure increasing from 4 to 600 kPa, the resistance dramatically decreased and finally reached a plateau (Figure 3d). We next measured the sensing behavior of flexible tactile sensors. The flexible tactile sensors revealed linear *I*–*V* curves (Figure 3e). It was found that as the pressure increased from 4 to 500 kPa, the resistance of the flexible tactile sensors decreased from 4678 to 418 Ω. This was associated with the change in contact area between electrode and MPs,[22] because upon applying pressure, CNTs between MPs were forced to pack more closely, resulting in increased electrical conduction pathways. In addition, the sensitivity of human skin is very significant. It was reported that light touch perception of the human finger could distinguish between two surfaces with a texture difference of less than 13 nm.[42] Therefore, the sensitivity is probably the most important factor in electronic skin. The printed tactile sensors exhibited ultrahigh sensitivity. With the decreasing of pressure, the sensitivity of the printed tactile sensors increased. The sensitivity can be ultimately improved to 2.08 kPa^{-1} at a light pressure as low as 0.12 kPa (Figure 3f), suggesting our tactile sensor had the potential to mimic the light touch sensation behavior of human skin. Study on the influence of the thickness on the sensitivity (Figure S6, Supporting Information) indicated that with the increasing of the thickness, the sensitivity of the tactile sensor slightly decreased. In addition, we also measured the resistance of the sensor with different moisture content and it showed that with the increasing of the moisture content, the sensitivity also slightly decreased (Figure S7, Supporting Information).

Our tactile sensor exhibited outstanding performance with low hysteresis (**Figure** 4b), reproducible cycling more than 8000 cycles (Figure 3g) and the results were consistent at a range of force speed. Moreover, SEM images (inset of Figure 3g) of the surface of the active layer before and after 8000 cycle testing showed that there were no cracks on the surface of the active layer of the sensor, indicating a good durability of the designed device. In addition, the performance of tactile sensor was highly reproducible. In particular, the respond time of tactile sensor was below 50 ms, which was similar to that of human skin as well (conduction velocity of meissner corpuscle is ≈35–70 ms).[42]

It is reported that tactile sensation is determined by the subsurface stresses and strains at the location of the mechanoreceptors in the skin, which is influenced by sliding interactions between skin and surfaces.[43] Therefore, we assessed the response of the tactile sensor to sliding force as well. As indicated in the literature that for tactile sensation, the normal force and sliding velocity normally employed by the consumer to judge a surface during finger sliding tests are 0.2–1.0 N and 10–60 mm s^{-1}, respectively.[44] To mimic the real human touch conditions, we used a 10 mm diameter nylon probe sliding on the sensor under 0.5 N normal load. It was found that the relative voltage changes were response sensitive under 0.5 and 1 Hz cyclic applied shearing force, respectively. Under 0.5 N normal load, with the increasing of shearing force from 0 to 0.2 N, the resistance of the tactile sensor decreased (Figure 3h,i). The sensing mechanism was due to force-dependent contact between CNTs on the surface of the MPs and the interdigitated electrode. With the increasing of the shearing force, the resultant force on the printed tactile sensors increased, resulting in decreasing of the distance of CNTs between MPs and increasing of the contact area between MPs and electrode, so that the electrical conduction pathways increased and resistance decreased. Therefore, to analyze the force distribution on the printed tactile sensor, we created and meshed the flexible 3D tactile sensor model for conducting a finite element analysis under shearing loading conditions. The model was found to accurately fit the force distribution of the sensor (Figures S8 and S9, Supporting Information).

To compare the output voltage signals with the pressure inputs, we mounted the tactile sensor on a multiaxis force/torque transducer (ATI Industrial Automation, Apex, NC, USA) as shown in the inset of Figure 4a, to measure the normal force in the *z*-direction generated by pressing the finger on the tactile sensor. It was found that the voltage waves were almost the same as the input pressure waves (Figure 4a). Considering the application, we mounted the tactile sensor on a mouse and a keyboard (Figure 4c,d) and attached the tactile sensor to the joint of hand (Figure 4e,f) for monitoring sensor response to movements. It was found that the response of sensor showed up outstanding reproducibility and stability when pressing on the keyboard and making bending motions of hand. These results provided a concept of monitoring varying degrees of motion by the flexible tactile sensor.

3. Conclusions

In conclusion, we have described a novel method to prepare a new type of piezoresistive sensors that were 3D printed by a new type of 3D printing ink. Our results clearly demonstrated that the MPs structure enabled the electronic skin to improve the sensitivity effectively. The response of the electronic skin to shearing forces was evaluated by simulating the touch behavior of human skin, and it was found that the response of tactile sensors was very sensitive under the applied shearing force. Particularly, the sensitivity of the flexible tactile sensor was significantly increased by the interconnected PDMS MPs and CNTs, with the sensitivity up to 2.08 kPa^{-1}, and with short response time (50 ms), high durability (over 8000 times), and flexibility. Moreover, the mechanical properties of the electronic skin were similar to that of human skin, thus the developed electronic skin can adapt to the skin strain associated with physical movement as wearable electronics. We expect

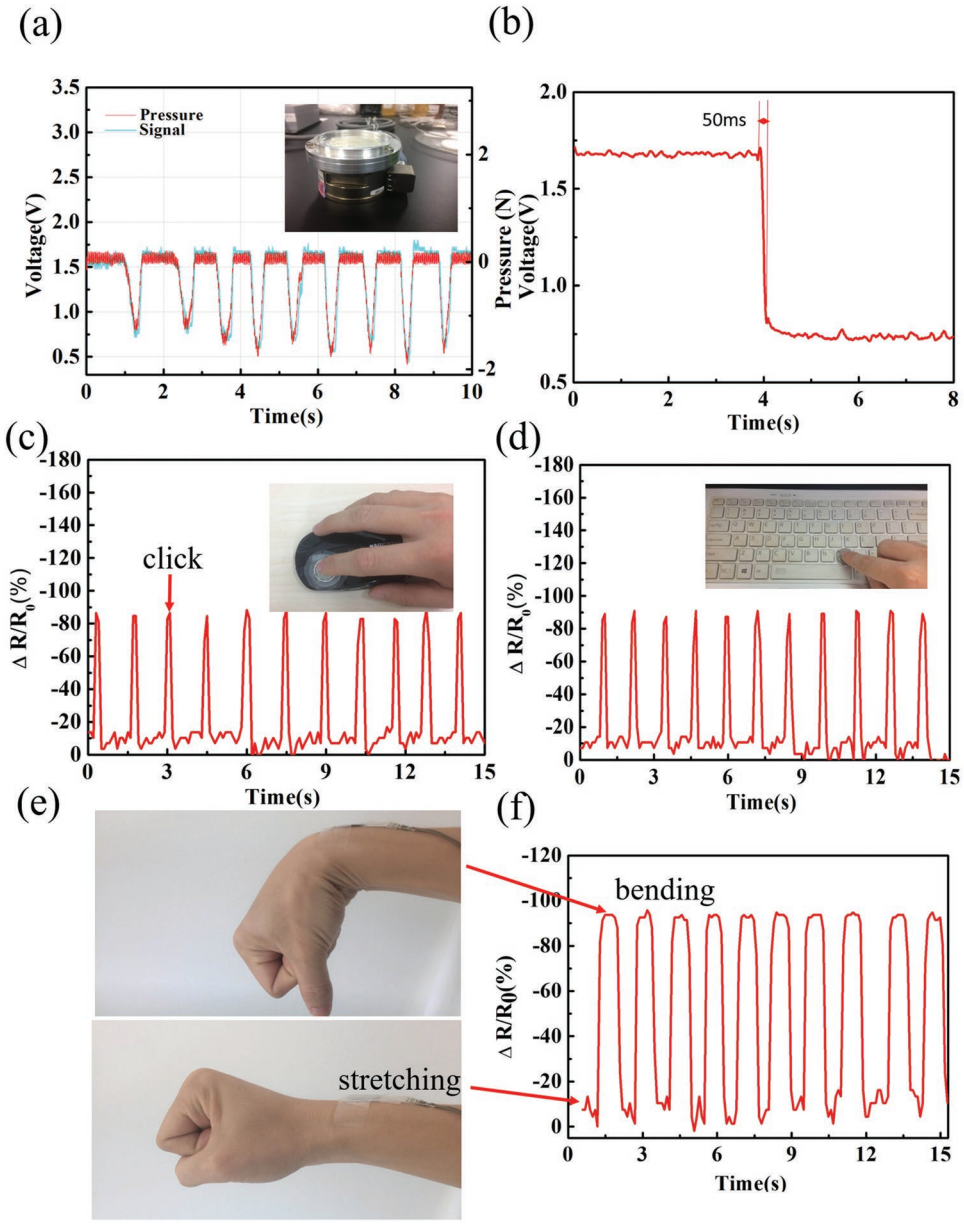

Figure 4. Applications of mechanical sensing of the flexible tactile sensor. a) Output signal and pressure as the function of time. b) Instant response of the tactile sensor, which exhibited response times of 50 ms. c) Click the mouse and d) keyboard. e) Attached the tactile sensor to the joint of hand. f) Resistance change signal of the tactile sensor to dynamic unloading and loading cycles in stretching and bending.

that the 3D printed flexible tactile sensor in this work could be used in various engineering applications such as skin patch sensor networks and implantable biomedical devices. In our future work, we will systematically research on the sensing and tribological behavior of the device with different microstructures, and the device design regarding miniaturization and scalability.

4. Experimental Section

PDMS-CNTs Composite Liquid Precursor: PDMS-CNTs composite liquid precursor was performed in two steps: 1) 500 mg multiwalled CNTs (DK Nano China, length 10–30 µm, diameter < 50 nm, purity > 98%) were blended with 4, 4.5, 5, 5.5 g PDMS base (Sylgard 184, Dow Corning, USA) and dispersed in ethyl acetate, respectively; 2) the mixed solution was heated at 80 °C for 5 h to obtain PDMS-CNTs composite liquid precursor by evaporating the ethyl acetate solvent completely.

Synthesis of PDMS MPs: First, 1:10 curing agents and PDMS precursors were degassed and mixed in a centrifugal mixer. Then, 6 mL of the PDMS precursors and curing agent mixture, and 30 mL of 8 wt% carboxylation chitosan (Sinopharm Chemical Reagent Co. Ltd., China) aqueous solution were mixed by a centrifugal mixer and a homogenizer at 3000 rpm subsequently to make an emulsion. Then poured PDMS emulsions into water at 85 °C and stirred for 2 h to prepare PDMS MPs. Second, 50 mL of aqueous solution of polysorbate 20 (0.1 wt%, Sinopharm Chemical Reagent Co. Ltd., China) was used for rinsing PDMS MPs ten times for further use.

Preparation of Elastomeric 3D Printing Inks: 1:10 curing agents and PDMS-CNTs composite liquid precursor were mixed by a centrifugal mixer, and then PDMS MPs were added with mechanical stir to make them adequately blend together. Then the inks were further blended by the homogenizer at 6×10^3 rpm for 10 min to obtain a homogenous 3D printing inks which exhibited gel-like behaviors, with about 20 wt% water in it at this moment.

Tactile Sensor 3D Printing: The 3D structure of the active layer of the tactile sensor for 3D printing was designed by 3D MAX 2016. The active layer of tactile sensor with the diameter of 20 mm and the height of 0.3 mm was printed within 2 min and cured at 60 °C for 5 h, and the water within it was evaporated completely in a drying oven.

Mechanical and Sensing Behavior Testing: The mechanical properties of the printed tactile sensor shown in Figure 2 were studied using a dynamic mechanical analyzer (DMA242E, Netzsch). In the pressure-sensing process (Figure 3d,f,g), the loading/unloading speed was 10 μm s^{-1}. In Figure 3h, the sliding tests were conducted by using a friction tester (UMT-tribolab, Germany). A 10 mm diameter nylon probe was sliding on the sensor under 0.5 N normal load with 0.5 and 1.0 Hz frequency, respectively, and a stroke of 5 mm. The experimental data on the electrical properties of the printed tactile sensors were collected from the oscilloscope. The microstructures of the active layer of the electronic skin were investigated by SEM. The microstructures of PDMS emulsion were investigated by an optical microscope. Signed consent was obtained from the subject for the experiment.

Supporting Information

Supporting Information is available from the Wiley Online Library or from the author.

Acknowledgements

The authors are grateful to the Shanghai Natural Science Foundation (grant no. 17ZR1442100) and National Natural Science Foundation of China (grant no. 21703279) for the financial support.

Conflict of Interest

The authors declare no conflict of interest.

Keywords

3D printing, microstructures, shearing forces, tactile sensors

Received: February 17, 2019
Revised: April 4, 2019
Published online: May 27, 2019

[1] M. Amjadi, K. Kyung, I. Park, M. Sitti, *Adv. Funct. Mater.* **2016**, *26*, 1678.
[2] K. Chen, W. Gao, S. Emaminejad, S. Emaminejad, D. Kiriya, H. Ota, H. Y. Nyein, K. Takei, A. Javey, *Adv. Mater.* **2016**, *28*, 4397.
[3] S. Choi, H. Lee, R. Ghaffari, T. Hyeon, D. Kim, *Adv. Mater.* **2016**, *28*, 4203.
[4] M. L. Hammock, A. Chortos, B. C. K. Tee, J. B. H. Tok, Z. Bao, *Adv. Mater.* **2013**, *25*, 5997.
[5] Y. S. Rim, S. H. Bae, H. Chen, N. D. Marco, Y. Yang, *Adv. Mater.* **2016**, *28*, 4415.
[6] Y. Zang, F. Zhang, C. Di, D. Zhu, *Mater. Horiz.* **2015**, *2*, 140.
[7] R. H. Friend, R. W. Gymer, A. B. Holmes, J. H. Burroughes, R. N. Marks, C. Taliani, D. D. C. Bradley, D. A. D. Santos, J. L. Brédas, M. Lögdlund, W. R. Salaneck, *Nature* **1999**, *397*, 121.
[8] S. I. Park, Y. Xiong, R. H. Kim, P. Elvikis, M. Meitl, D. H. Kim, J. Wu, J. Yoon, C. J. Yu, Z. Liu, *Science* **2009**, *325*, 977.
[9] Y. Honmou, S. Hirata, H. Komiyama, J. Hiyoshi, S. Kawauchi, T. Iyoda, M. Vacha, *Nat. Commun.* **2014**, *5*, 4666.
[10] A. Haeberlin, A. Zurbuchen, S. Walpen, J. Schaerer, T. Niederhauser, C. Huber, H. Tanner, H. Servatius, J. Seiler, H. Haeberlin, J. Fuhrer, R. Vogel, *Heart Rhythm* **2015**, *12*, 1317.
[11] C. Yu, C. Masarapu, J. Rong, B. Wei, H. Jiang, *Adv. Mater.* **2009**, *21*, 4793.
[12] K. Song, J. H. Han, T. Lim, N. Kim, S. Shin, J. Kim, H. Choo, S. Jeong, Y. C. Kim, Z. L. Wang, *Adv. Healthcare Mater.* **2016**, *5*, 1572.
[13] C. Dagdeviren, P. Joe, O. L. Tuzman, K. Park, K. J. Lee, Y. Huang, J. A. Rogers, *Extreme Mech. Lett.* **2016**, *9*, 269.
[14] C. Dagdeviren, Z. Li, Z. L. Wang, *Annu. Rev. Biomed. Eng.* **2017**, *19*, 85.
[15] T. Sekitani, H. Nakajima, H. Maeda, T. Fukushima, T. Aida, K. Hata, T. Someya, *Nat. Mater.* **2009**, *8*, 494.
[16] R.-H. Kim, D.-H. Kim, J. Xiao, B. H. Kim, S.-I. Park, B. Panilaitis, R. Ghaffari, J. Yao, M. Li, Z. Liu, V. Malyarchuk, D. G. Kim, A.-P. Le, R. G. Nuzzo, D. L. Kaplan, F. G. Omenetto, Y. Huang, Z. Kang, J. A. Rogers, *Nat. Mater.* **2010**, *9*, 929.
[17] R.-H. Kim, M.-H. Bae, D. G. Kim, H. Cheng, B. H. Kim, D.-H. Kim, M. Li, J. Wu, F. Du, H.-S. Kim, S. Kim, D. Estrada, S. W. Hong, Y. Huang, E. Pop, J. A. Rogers, *Nano Lett.* **2011**, *11*, 3881 .
[18] M. L. Hammock, A. Chortos, B. C. K. Tee, J. B. H. Tok, Z. N. Bao, *Adv. Mater.* **2013**, *25*, 5997.
[19] T. Q. Trung, N. E. Lee, *Adv. Mater.* **2016**, *28*, 4338.
[20] Y. Zang, F. Zhang, D. Huang, X. Gao, C. A. Di, D. Zhu, *Nat. Commun.* **2015**, *6*, 6269.
[21] S. C. B. Mannsfeld, B. C. K. Tee, R. M. Stoltenberg, C. V. H. H. Chen, S. Barman, B. V. O. Muir, A. N. Sokolov, C. Reese, Z. Bao, *Nat. Mater.* **2010**, *9*, 859.
[22] C. L. Choong, M. B. Shim, B. S. Lee, S. Jeon, D. S. Ko, T. H. Kang, J. Bae, S. H. Lee, K. E. Byun, J. Im, Y. J. Jeong, C. E. Park, J. J. Park, U. I. Chung, *Adv. Mater.* **2014**, *26*, 3451.
[23] Y. Wei, S. Chen, F. Li, Y. Lin, Y. Zhang, L. Liu, *ACS Appl. Mater. Interfaces* **2015**, *7*, 14182.
[24] M. Kumar, H. Bhaskaran, *Nano Lett.* **2015**, *15*, 2562.
[25] L. Persano, C. Dagdeviren, Y. Su, Y. Zhang, S. Girardo, D. Pisignano, Y. Huang, J. A. Rogers, *Nat. Commun.* **2013**, *4*, 1633.
[26] D. J. Lipomi, M. Vosgueritchian, B. C. Tee, S. L. Hellstrom, J. A. Lee, C. H. Fox, Z. Bao, *Nat. Nanotechnol.* **2011**, *6*, 788.
[27] M. Ramuz, B. C. Tee, J. B. Tok, Z. Bao, *Adv. Mater.* **2012**, *24*, 3223.
[28] F. R. Fan, L. Lin, G. Zhu, W. Wu, R. Zhang, Z. L. Wang, *Nano Lett.* **2012**, *12*, 3109.
[29] X. Wang, Y. Gu, Z. Xiong, Z. Cui, T. Zhang, *Adv. Mater.* **2014**, *26*, 1336.
[30] C. F. Hu, *J. Micromech. Microeng.* **2011**, *21*, 115012.
[31] C. F. Hu, J. Y. Wang, Y. C. Liu, M. H. Tsai, W. Fang, *Nanotechnology* **2013**, *24*, 444006.
[32] B. W. Zhu, Z. Q. Niu, H. Wang, W. R. Leow, H. Wang, Y. G. Li, L. Y. Zheng, J. Wei, F. W. Huo, X. D. Chen, *Small* **2014**, *10*, 3625.
[33] C. Pang, G. Y. Lee, T. I. Kim, S. M. Kim, H. N. Kim, S. H. Ahn, K. Y. Suh, *Nat. Mater.* **2012**, *11*, 795.
[34] S. Gong, W. Schwalb, Y. Wang, Y. Chen, Y. Tang, J. Si, B. Shirinzadeh, W. Cheng, *Nat. Commun.* **2014**, *5*, 3132.
[35] C. B. Huang, S. Witomska, A. Aliprandi, M. A. Stoeckel, M. Bonini, A. Ciesielski, P. Samorì, *Adv. Mater.* **2019**, *31*, 1804600.

[36] L. J. Pan, A. Chortos, G. H. Yu, Y. Q. Wang, S. Isaacson, R. Allen, Y. Shi, R. Dauskardt, Z. N. Bao, *Nat. Commun.* **2014**, *5*, 3002.
[37] J. U. Lind, T. A. Busbee, A. D. Valentine, F. S. Pasqualini, H. Yuan, M. Yadid, S. J. Park, A. Kotikian, A. P. Nesmith, P. H. Campbell, J. J. Vlassak, J. A. Lewis, K. K. Parker, *Nat. Mater.* **2017**, *16*, 303.
[38] S. Z. Guo, K. Qiu, F. Meng, S. H. Park, M. C. McAlpine, *Adv. Mater.* **2017**, *29*, 1701218.
[39] H. Wei, K. Li, W. G. Liu, H. Meng, P. X. Zhang, C. Y. Yan, *Adv. Eng. Mater.* **2017**, *19*, 1700341.
[40] S. Roh, D. P. Parekh, B. Bharti, S. D. Stoyanov, O. D. Velev, *Adv. Mater.* **2017**, *29*, 1701554.
[41] F. Khatyr, C. Imberdis, P. Vescovo, D. Varchon, J.-M. Lagarde, *Skin Res. Technol.* **2004**, *10*, 96.
[42] E. R. Kandel, J. H. Schwartz, T. M. Jessell, S. A. Siegelbaum, A. J. Hudspeth, *Principles of Neural Science*, McGraw-Hill, New York, NY, USA **2012**.
[43] A. Zimmerman, L. Bai, D. D. Ginty, *Science* **2014**, *346*, 950.
[44] A. M. Smith, S. H. Scott, *J. Neurophysiol.* **1996**, *75*, 1957.